Masroor M. Shakir
Burhan N. Qazi
Rafik A. Mardshah

Department of Physics,
Faculty of Science,
Jumar Tabeer University,
Rawalpindi, Pakistan

Fundamentals of Microwave Integrated Circuits Based on High-Temperature Superconductors

A brief review is given of recent publications showing that the applications of high-temperature superconductors (HTS) in microwave technologies have become an integral part of industrial business. The basic components of microwave devices are HTS epitaxial films on dielectric substrates. It is shown that the properties of interfaces between the substrates and HTS films are crucially important for obtaining high-quality HTS films. The change of the structure in the process of film growth is related to the initial stage of HTS nucleation at the interface between the substrate and the film. The film surface resistance at microwave frequencies depends on the HTS film structure. It is known that one can decrease the surface resistance, which will permit designing higher-quality microwave-microelectronics components to operate at cryogenic temperatures by improving the film structure. A discussion is given how to improve the HTS film microwave properties to make possible industrial production of high-performance HTS devices and subsystems.

***Keywords*:** HTS, Superconductivity, High temperatures, Integrated circuits
Received: 5 May 2013, **Accepted:** 12 June 2013

1. Introduction

Microwave microelectronics is the most rapidly growing branch of the modern electronics that is connected with the development of telecommunication systems, such as TV satellite broadcasting, cellular communications, and various global navigation systems. Insertion loss requirements in some of these applications make the use of high-temperature superconductors (HTS) an attractive alternative to most of the traditional technologies [1]. The use of HTS thin-film structures in microwave integrated circuits (MIC) employed widely in space applications and mobile communication base stations offers a possibility of reducing markedly the weight and volume of the microwave equipment, although the system must certainly include cryogenic equipment providing the operational temperature in the range from 60 to 77 K. In this context, it is appropriate to mention the successful testing of a microwave HTS filter under space-flight conditions in the framework of High-Temperature Superconductor Space Experiment-II (HTSSE-II) [2], as well as the Superconductor Communications Systems (SUCOMS) Project [3], which is funded by the European Program of the Advanced Communications Technologies and Services. Thus one can say that the HTS applications in microwave engineering have become a part of industrial business. This stresses the importance of investigation of the physical properties of HTS thin films and of the development of recommendations for improving the microwave characteristics of such films. Thin HTS films are prepared by epitaxial growth on single-crystal dielectric substrates. In many cases, the film quality is governed to a considerable extent by the processes occurring at the interface between the film and the substrate. As a consequence, the state of the interface in heteroepitaxial systems consisting of HTS films and dielectric substrates becomes extremely important from the standpoint of practical applications of HTS in modern microwave electronics. It should also be noted that the extremely narrow-band planar filters which are going to be used in telecommunication systems can be realized only on the basis of HTS film structures, since common conducting materials cannot provide the required low value of the surface resistance.

2. High-Temperature Superconductors (HTS)

Superconductivity was discovered in 1911. The highest superconducting-transition temperature observed in the Nb_3Ge compound did not rise above 23.2 K until 1986, when possible superconductivity in the La-Ba-Cu-O ceramic was announced. Before the high-temperature superconductivity has been established to exist, the oxide-type superconductors were considered as nothing else but a strange phenomenon being not worthy of a serious consideration.

In the beginning of 1987,the situation changed abruptly, and the HTS became a subject of worldwide interest. Fig. 1 displays the history of high-temperature superconductors. A more detailed information is given in Table 1 [4]. As the initial

 All Rights Reserved

agitation and euphoria gradually died out, the realistic area of HTS applications has been revealed. The $YBa_2Cu_3O_{7-x}$ and $Tl_2Ba_2Ca_2Cu_3O_{10}$ compounds were found suitable for practical applications as a basis of microwave devices [5,6].

Table (1) High-temperature superconductor transition temperature records through the years

Material	T_c, K	**Year**
$Ba_xLa_{5-x}Cu_5O_y$	30 - 35	1986
$YBa_2Cu_3O_{7-\delta}$	91 - 93	1987
$Bi_2Sr_2Ca_2Cu_3O_{10}$	106 - 110	1988
$Tl_2Ba_2Ca_2Cu_3O_{10}$	125	1988
$Tl_2Ba_2Ca_2Cu_3O_{10}$ (at 7 GPa)	131	1993
$HgBa_2Ca_2Cu_3O_{8+\delta}$	133	1993
$HgBa_2Ca_2Cu_3O_{8+\delta}$ (at 25 GPa)	155	1993
$Hg_{0.8}Pb_{0.2}Ba_2Ca_2Cu_3O_x$	133	1994
$HgBa_2Ca_2Cu_3O_{8+\delta}$ (at 30 GPa)	164	1994

HTS materials were initially obtained in the form of ceramic pellets. HTS materials are still being referred to as ceramics. Fig. 2 illustrates the structure of a polycrystalline ceramic sample. The high resistance of the inter-granular contacts degrades the electrical properties of HTS materials. This is why the HTS ceramics do not enjoy practical applications in modern high-frequency electronics.

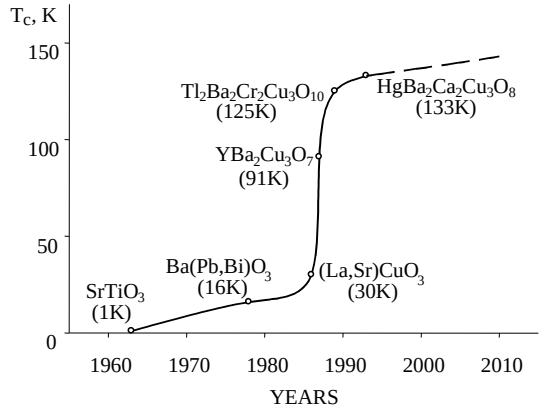

Fig. (1) Progress in high-temperature superconductivity

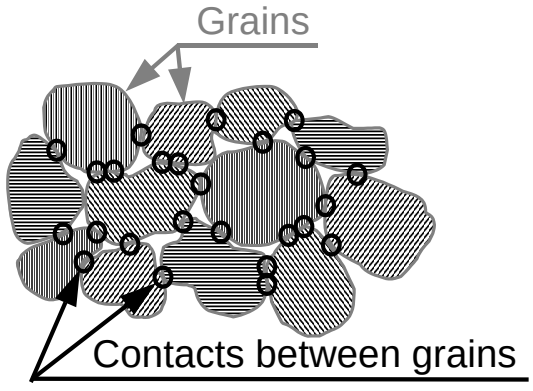

Fig. (2) Structure of a polycrystalline ceramic sample

While HTS materials are grown presently in the form of perfect single crystals and used in investigation of the fundamental properties of substances, no devices have yet been designed on the basis of HTS single crystals. The use of HTS in electronics is currently limited to thin films on a dielectric substrate. In the case of microwave applications, the best substrate for $YBa_2Cu_3O_{7-x}$ films was found to be the *r*-cut sapphire buffered by a thin CeO_2 layer [7,8] (Fig. 3). The thickness of the substrate is typically 500 μm, that of the buffer layer, 0.05 μm, and the film is 0.2 – 1.0 μm thick. The problem of growing perfect HTS epitaxial films has not been solved satisfactorily. Fig. 4 illustrates possible formation of $YBa_2Cu_3O_{7-x}$ grains on a crystalline substrate, where (a) is an epitaxial *c*-axis HTS grain, (b) is an *a*-axis HTS grain, and (c) is an axially misaligned HTS grain.

3. Experimental Part

The surface resistance of HTS at microwave frequencies is responsible for the loss in planar transmission lines and for the decay of oscillation in resonators, and, consequently, for the resulting Q-factor of filters and multiplexers.

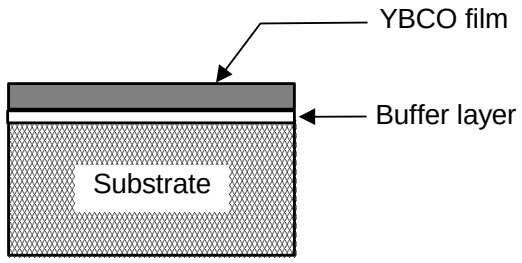

Fig. (3) CeO_2-buffered $YBa_2Cu_3O_{7-x}$ film on an *r*-cut sapphire substrate. Thickness of the substrate is 500 μm, that of the buffer layer is 0.05 μm, and the film thickness ranges from 0.2 to 1.0 μm.

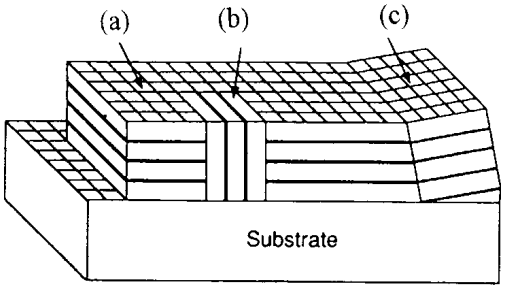

Fig. (4) $YBa_2Cu_3O_{7-x}$ grains on crystalline substrate: (a) epitaxial *c*-axis HTS grain, (b) *a*-axis HTS grain, and (c) axially misaligned HTS grain

Figure (5) shows experimental data on the surface resistance of (a) HTS and (b) copper samples as a function of frequency obtained at a temperature T = 77 K [9]. The advantage of HTS over copper is obvious. The higher slope compared to that of the copper sample characterizes the frequency dependence of the HTS surface resistance, which

© Iraqi Society for Alternative and Renewable Energy Sources and Techniques (I.S.A.R.E.S.T.)

directly follows from the electrodynamics of a superconductor material.

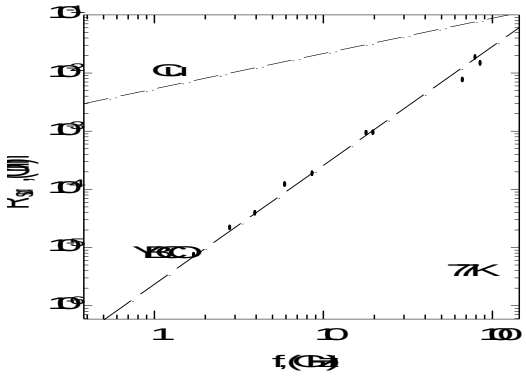

Fig. (5) Surface resistance of (a) HTS and (b) copper samples as a function of frequency at T = 77 K

The surface impedance of an HTS material for a plane electromagnetic wave incident normally to its surface is defined as the ratio of $|\boldsymbol{E}|$ to $|\boldsymbol{H}|$ on the surface of the sample. It is described by the equation

$$Z_{sur} = R_{sur} + iX_{sur} = \left(\frac{i\omega\mu_0}{\sigma_1 - i\sigma_2} \right)^{1/2} \quad (1)$$

where R_{sur} and X_{sur} are the surface resistance and the surface reactance, correspondingly, $\omega=2\pi f$, f is the frequency, μ_0 is the magnetic permeability of free space, and σ_1 and σ_2 are the real and imaginary parts of the conductivity.

The two-fluid model proposed by Gorter and Casimir [10] is commonly used for a realistic description of the HTS surface impedance [5,6]. In accordance with this model, the components of the conductivity can be written as

$$\sigma_1 = \frac{e^2 n_n \tau}{m} \cdot \frac{1}{1+(\omega\tau)^2} \quad (2)$$

$$\sigma_2 = \frac{e^2 n_s}{\omega m} \cdot \left[1 + \frac{n_n}{n_s} \cdot \frac{\omega\tau}{1+(\omega\tau)^2} \right] \quad (3)$$

where e and m are the charge and the effective mass of the electron, respectively, τ is the relaxation time, and n_n and n_s are the densities of the normal and superconducting charge carriers.

Within the microwave frequency range [$(\omega\tau)^2 << 1$], equations (2) and (3) can be simplified to

$$\sigma_1 = \frac{e^2 n_n \tau}{m}, \quad (4)$$

$$\sigma_2 = \frac{1}{\omega\mu_0\lambda_L^2}, \quad (5)$$

where

$$\lambda_L = \left(\frac{e^2 n_s \mu_0}{m} \right)^{-1/2} \quad (6)$$

λ_L is the London penetration depth.

Substituting (4) and (5) into equation (1) and taking into account that for $T<T_c$ the inequality $\omega\mu_0\sigma_n\lambda_L^2 << 1$ is valid, one obtains [5, 6]:

$$R_{sur} = \frac{1}{2}(\omega\mu_0)^2 \sigma_n \lambda_L^3, \quad (7)$$

$$X_{sur} = \omega\mu_0\lambda_L. \quad (8)$$

The characteristics σ_n and λ_L are temperature dependent. The quadratic frequency dependence of the microwave surface resistance (7) was confirmed experimentally (Fig. 5).

If the thickness of an HTS sample in the wave propagation direction is comparable with the London penetration depth, the interference of the waves reflected from the two sides of the sample should be taken into account. In this case, the surface impedance (1) should be recast in the following form

$$Z_{sur} = \frac{R_{sur} + iX_{sur}}{\tanh(ikd)}, \quad (9)$$

where d is the film thickness, and k is the complex wave number [11]. Using (7)-(9), one obtains after some transformations

$$R_{sur} = (\omega\mu_0)^2 \sigma_n \frac{\lambda_L^4}{d}, \quad (10)$$

$$X_{sur} = \omega\mu_0 \frac{\lambda_L^2}{d} \quad (11)$$

The equations (10) and (11) are valid, if $d > 2\lambda_L$. Otherwise, equations (7) and (8) should be used. Figure (6) illustrates the dependence of the surface resistance of an HTS film on normalized film thickness. In order to obtain the smallest possible value of the surface resistance of a film, the film thickness should be $d > 2\lambda_L$. This requirement leads to a film thickness of about 1 μm.

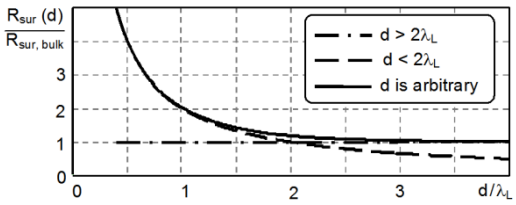

Fig. (6) Surface resistance of an HTS film as a function of normalized film thickness

In most of the HTS film growth technologies, the structure of the film changes during the growth process. Figure (7) illustrates the change in the crystal structure of a spontaneously oriented $YBa_2Cu_3O_{7-x}$ film on a single crystal substrate. A disordered layer is characterized by a larger London penetration depth than a perfectly oriented film (Fig. 8). Therefore a thicker disoriented layer has a higher surface resistance than a thinner but a highly oriented film. Somewhere in between lies the critical

 All Rights Reserved

film thickness, which corresponds to the minimum of the surface resistance Somewhere in between lies the critical film thickness, which corresponds to the minimum surface resistance (Fig. 9). This phenomenon was experimentally observed and theoretically explained [12]. The reflection electron diffraction patterns and electron micrographs made on $YBa_2Cu_3O_{7-x}$ films of different thicknesses confirmed that the layer structure changes in the course of film growth. The existence of a surface resistance minimum and the measured critical film thickness have been confirmed in an independent experiment [13].

An investigation of HTS film growth revealed that the change of the structure during the process is connected with the initial stage of nucleation of HTS nuclei at the interface between the substrate and the film [14, 15]. An improved regime of HTS film growth produced films with a perfect structure up to film thicknesses of 1 - 1.5 μm. Fig. 10 shows the temperature dependence of the surface resistance of $YBa_2Cu_3O_{7-x}$ films 400 nm and 550 nm thick obtained with an improved growing process [14].

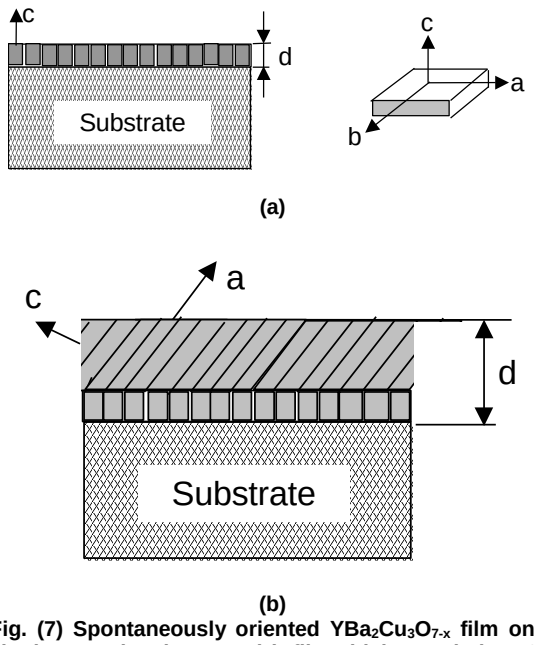

Fig. (7) Spontaneously oriented $YBa_2Cu_3O_{7-x}$ film on a single-crystal substrate: (a) film thickness below 0.3 μm, and (b) film thickness above 0.3 μm

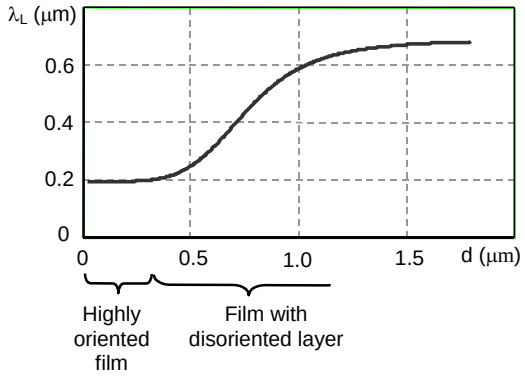

Fig. 8. Effective London penetration depth as a function of $YBa_2Cu_3O_{7-x}$ film thickness

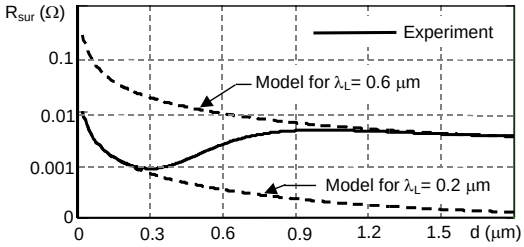

Fig. 9 Surface resistance of a $YBa_2Cu_3O_{7-x}$ film with a spontaneously organized structure

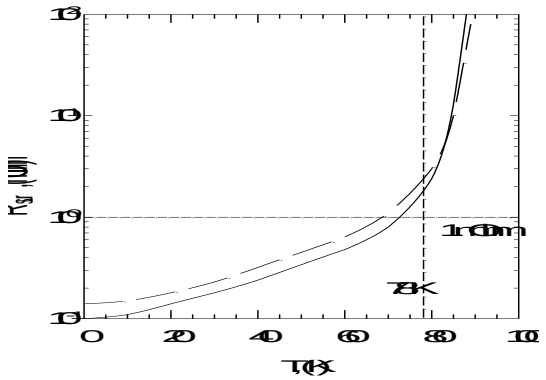

Fig. 10 Temperature dependence of the surface resistance of a $YBa_2Cu_3O_{7-x}$ film of thickness 400 nm (dashed line) and 550 nm (solid line)

Fairly simple expressions were derived to describe the temperature dependence of the surface impedance of thin HTS films using the following phenomenological model [11]:

$$R_{sur}(t)=\begin{cases}\dfrac{1}{\sigma_N(t)d} & \text{for} \quad t\geq 1 \quad (N-\text{state})\\ \dfrac{(\omega\mu_0)^2\sigma_N(t)}{1+[\omega\mu_0\sigma_N(t)\lambda_L^2(t)]^2}\cdot\dfrac{\lambda_L^4(t)}{d} & \text{for} \quad t<1 \quad (S-\text{state})\end{cases}, \tag{12}$$

$$X_{sur}(t)=\begin{cases}0 & \text{for} \quad t\geq 1 \quad (N-\text{state})\\ \omega\mu_0\cdot\dfrac{\lambda_L^2(t)}{d} & \text{for} \quad t<1 \quad (S-\text{state})\end{cases}, \tag{13}$$

where

© Iraqi Society for Alternative and Renewable Energy Sources and Techniques (I.S.A.R.E.S.T.)

$$\sigma_N(t)=\sigma_N(1)\begin{cases} t^{-1} \text{ for } \quad t \geq 1 \quad (\text{N-state}) \\ t^{\gamma-1}+\alpha\cdot(1-t^{\gamma}) \quad \text{for} \quad t<1 \quad (\text{S-state}) \end{cases}, \tag{14}$$

$$\left[\lambda_L(0)/\lambda_L(t)\right]^2 = 1-t^{\gamma}, \tag{15}$$

$$\lambda_L(0) = 0.13\cdot 10^{-6}\cdot\exp(1.27-0.5\gamma) \qquad [\text{m}], \tag{16}$$

$$t = T/T_C, \tag{17}$$

Here $\sigma_N(1)$ is the conductivity of normal charge carriers at the transition temperature T_C, $\lambda_L(0)$ is the London penetration depth at $T = 0$, α is the residual resistance parameter, and γ is an empirical parameter.

Equation (13) can be used to find the kinetic inductance of the film in the superconducting state:

$$L_k(t) = \mu_0\cdot\frac{\lambda_L^2(t)}{d} \tag{18}$$

The model of the surface impedance uses four fitting parameters, namely, the transition temperature T_C, the normal conductivity σ_N (1), the parameter γ, and the residual resistance parameter α. The model parameters can be extracted from the experimental characteristics of HTS films. The model parameter $\gamma = 1.5 – 2.5$ depends on the HTS film quality, more specifically, the higher the film quality, the larger is γ, and the lower is the microwave surface resistance of the film. The parameter γ is responsible for the temperature dependence of the London penetration depth and determines the slope of the temperature dependence of the surface resistance in the vicinity of the transition temperature. The residual resistance parameter α affects the limiting low-temperature surface resistance.

The validity of the model was verified using numerous experimental data [13, 16-25]. The modeling of the temperature dependence of the YBCO film surface impedance is compared with experimental results [23] in Fig. 11.

4. HTS Applications at Microwave Frequencies

The model described above is used as a Computer Aided Design (CAD) tool for designing MIC components and microwave subsystems. In order to ensure appropriate modeling of characteristics of HTS devices, the CAD programs should include as complete information as possible on the dielectric and thermal properties of the substrate material, thermal resistance of the interface between HTS film and substrate, etc.

For an accurate simulation of an HTS planar transmission line, one should take into account all specific characteristics of the superconducting material, such as the surface resistance, kinetic inductance, and the nonuniform current distribution over the cross-sectional area of the HTS planar line [11]. The characteristics mentioned are temperature dependent. The model of an HTS planar transmission line [11, 26] includes all these characteristics in the wave propagation parameters, namely, in the phase velocity and the attenuation coefficient of the electromagnetic wave in the line.

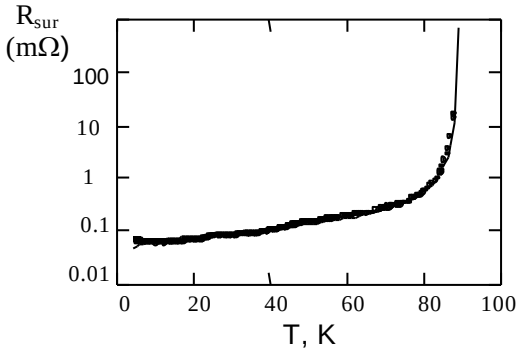

Fig. (11) Measured [22] (full circles) and simulated (solid line) temperature dependences of the surface resistance of a YBCO film on a sapphire substrate (f=9.5GHz). The model parameters used are: T_c=88K, $\sigma_n(1)=2.7\text{x}10^6$ (Ohm.m)$^{-1}$, α=3.1, and γ=1.95

High-performance narrowband filters have a considerable potential in the area of mobile communications. A number of versions of planar HTS filters have been recently proposed [3, 26-36]. The main advantage of the HTS filters consists in their extremely low in-band insertion loss level. Planar-structure filter configurations are characterized by a small size and weight. Development of such filters requires precise modeling which should take into consideration the HTS film contribution to the propagation parameters of the transmission line sections used as a basis for filter resonators. We employ the phenomenological description of the microwave surface impedance put forward in (12)-(18). It permits high-accuracy prediction of the HTS filter characteristics for any desired temperature. Figure (12a) illustrates a 10-pole filter [33, 35] based on a half-wavelength array of microstrip resonators. A comparison of the

 All Rights Reserved

simulated and measured characteristics shows them to be in a good agreement (Fig. 12b). Another filter structure (Fig. 13a) based on hairpin resonators [36] was also simulated with a high accuracy. The measured and simulated characteristics are presented in Fig. 13b.

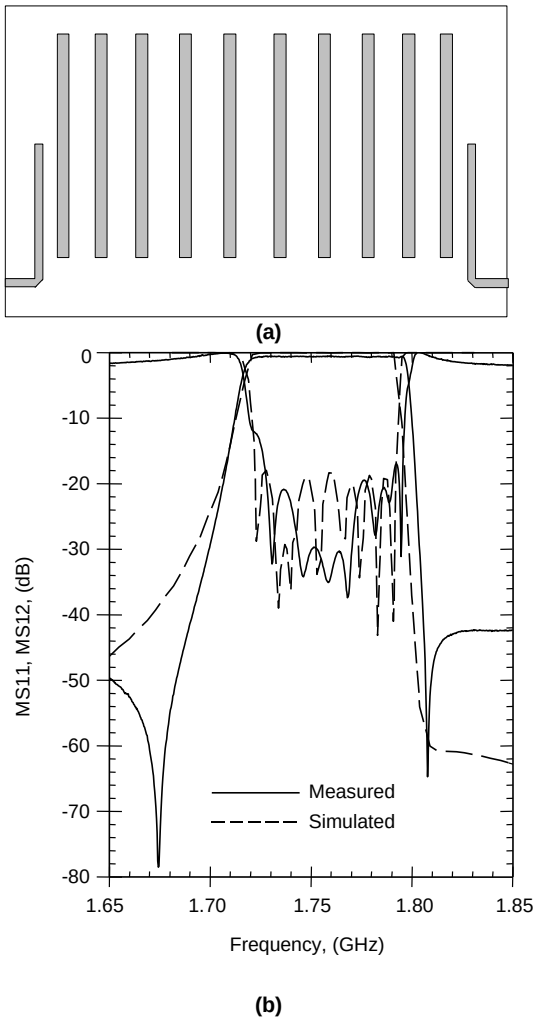

Fig. 12 10-pole filter on a $LaAlO_3$ substrate (T=77K): (a) layout, and (b) simulated and measured characteristics (shown with a dashed and a solid curve, respectively)

The design and testing of planar microwave filters makes often use of specially introduced trimmers [3,5,6]. Usually the trimmers are small dielectric screws. By properly rotating the screw, one can change the distance between the screw and a filter component. In this way the couplings between the filter components and their resonant frequencies can be varied so as to correct the filter characteristics. The trimming procedure is poorly suited for mass production of microwave components. In order to avoid trimming, a CAD system should be properly developed and carefully applied. This requires investigation of how the model parameters of the HTS microwave surface impedance affect the filter characteristics. It was found that the most important model parameters are γ and the residual resistance parameter α. In order to provide an accurate simulation of the filter designed, it is necessary to find these parameters from HTS film measurements. Another important characteristic is the HTS film thickness; indeed, the thicker the film, the less influence it exerts on the filter parameters.

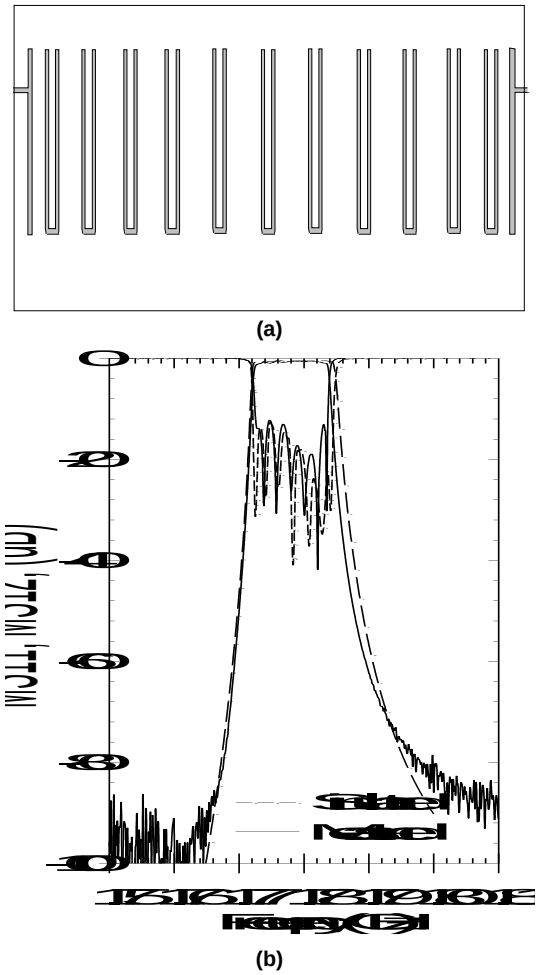

Fig. (13) 11-pole filter on a $LaAlO_3$ substrate (T=65K): (a) layout, and (b) simulated and measured characteristics (shown by a dash and a solid curve, respectively)

The substrate thickness and the dielectric permittivity of the substrate material are also of a considerable importance for the design procedure. In designing trimmingless filters, the following characteristics are to be kept within required limits: the parameter γ, the residual resistance parameter α, and the thickness of the HTS film, as well as the dielectric permittivity and the thickness of the dielectric substrate. After these parameters have been certified, one can directly approach the problem of mass production of high-quality trimmingless HTS filters. The crucial point in trimmingless filter design and production is a reproducible technological process providing high quality HTS film growth.

© Iraqi Society for Alternative and Renewable Energy Sources and Techniques (I.S.A.R.E.S.T.)

5. Conclusion

The potential of HTS epitaxial films (neither ceramics nor single crystals) on dielectric substrates for use in MIC components and microwave subsystems is growing. The design and investigation of high-quality prototypes of HTS planar microwave devices have demonstrated good prospects for HTS applications at microwave frequencies. The properties of the interface between the substrate and the HTS film are of crucial importance for obtaining HTS films of a high quality. Considerable effort is being expended in trying to obtain high quality HTS epitaxial films. Valuable experience is gained, which will prove useful for developing the technology of preparation of other oxide materials, particularly, for obtaining high quality ferroelectric films.

References

[1] *Special Issue on the Microwave and Millimeter Wave Applications of High Temperature Superconductivty, IEEE Trans. on MTT* **44** (1996) 1193.

[2] M. Nisenoff, in *4th European Conf. on Applied Superconductivity* (Barcelona, Spain, Sept. 1999).

[3] J.-S. Hong et al., *IEEE Trans. on MTT* **47** (1999) 1656.

[4] C. Poole, H. Farach and R. Creswick, **"Superconductivity",** (Academic Press, 1995).

[5] Z.-Y. Shen, **"High-Temperature Superconducting Microwave Circuits",** (Artech House, Boston-London, 1994).

[6] M.J. Lancaster, **"Passive Microwave Device Applications of High-temperature Superconductors",** (Cambridge University Press, 1997).

[7] I.B. Vendik et al., *Intern. J. of Microwave and Millimiter-Wave CAE* **4** (1994) 374.

[8] E.K. Hollmann et al., *Supercond. Sci. Technol.,* **7** (1994) 609.

[9] H. Piel and G. Mueller, *IEEE Trans. Magn.* **27** (1991) 854.

[10] C.S. Gorter and H. Casimir, *Phys. Z.* **35** (1934) 963.

[11] O.G. Vendik, I.B. Vendik and D.I. Kaparkov, *IEEE Trans. on Microwave Theory and Techniques* **46** (1998) 469.

[12] O.G. Vendik et al., *Physica C* **C179** (1991) 91.

[13] A. Mogro-Campero et al., *J. Appl. Phys.* **73** (1993) 5295.

[14] A.G. Zaitsev et al., *Phisica C* **C264** (1996) 125.

[15] E.K. Hollmann et al., *Technical Phys. Lett.,* **23** (1997) 186.

[16] J. Gao et al., *J. Appl. Phys.* **71** (1992) 2333.

[17] N. Klein et al., *J. Superconductivity* **5** (1992) 195.

[18] N. Klein et al., *IEEE Trans. Appl. Supercond.,* **3** (1993) 1102.

[19] W. Rauch et al., *J. Appl. Phys.* **73** (1993).

[20] A. Porch, M.J. Lancaster and R.G. Humphreys, *IEEE Trans on Microwave Theory and Techniques* **43** (1995) 306.

[21] E. Farber et al., *Eur. Phys. J. B.* **5** (1998) 159.

[22] I.B. Vendik, D.I. Kaparkov and A.A. Svishchev, *Microwave and Optical Technol. Lett.,* **16** (1997) 14.

[23] A.G. Zaitsev et al., *IEEE Trans. Appl. Superconductivity* **7** (1997) 1483.

[24] A.G. Zaitsev et al., *Appl. Phys. Lett* **75** (1999) 4165.

[25] Y. Kobayashi, in *Proc. 26th Eur. Microwave Conference* (Prague, 1996) 823.

[26] I.B. Vendik et al., *Superconductor Science and Technology* **12** (1999) 394.

[27] D. Zhang et al., *IEEE Microwave Guided-Wave Lett* **5** (1995) 405.

[28] G.-C. Liang et al., *Trans. Microwave Theory Tech.* **43** (1995) 3020.

[29] R.R. Mansour et al., *Trans. Microwave Theory Tech.* **44** (1996) 1213.

[30] S.H. Talisa et al., *Trans. Microwave Theory Tech.* **44** (1996) 1229.

[31] C. Rauscher, J.M. Pond and G.B. Tait, *Trans. Microwave Theory Tech.* **44** (1996) 1240.

[32] M.J. Lancaster et al., *Trans. Microwave Theory Tech.* **44** (1996) 1339.

[33] I.B. Vendik et al., *Technical Phys. Lett.,* **24** (1998) 968.

[34] A. Deleniv, V. Kondratiev and I. Vendik, *Electronics Lett.* **35** (1999) 405.

[35] I.B. Vendik et al., *IEEE Trans. Appl. Superconductivity* **9** (1999) 3577.

[36] H.T. Kim et al., *IEEE Trans. Appl. Superconductivity* **9** (1999) 3909.

 All Rights Reserved